Received: 6 October 2022 | Accepted: 18 November 2022

DOI: 10.1002/pamm.202200108

Scaled boundary isogeometric analysis with C^1 coupling for Kirchhoff-Love theory

Jeremias Arf[1,*], **Mathias Reichle**[2], **Sven Klinkel**[2], and **Bernd Simeon**[1]

[1] TU Kaiserslautern, Paul-Ehrlich-Straße 31, 67663 Kaiserslautern
[2] RWTH Aachen, Mies-van-der-Rohe-Str. 1, 52074 Aachen, Germany

Scaled boundary isogeometric analysis (SB-IGA) describes the computational domain by proper boundary NURBS together with a well-defined scaling center; see [5]. More precisely, we consider star convex domains whose domain boundaries correspond to a sequence of NURBS curves and the interior is determined by a scaling of the boundary segments with respect to a chosen scaling center. However, providing a decomposition into star shaped blocks one can utilize SB-IGA also for more general shapes. Even though several geometries can be described by a single patch, in applications frequently there appear multipatch structures. Whereas a C^0 continuous patch coupling can be achieved relatively easily, the situation becomes more complicated if higher regularity is required. Consequently, a suitable coupling method is inevitably needed for analyses that require global C^1 continuity.

In this contribution we apply the concept of analysis-suitable G^1 parametrizations [2] to the framework of SB-IGA for the C^1 coupling of planar domains with a special consideration of the scaling center. We obtain globally C^1 regular basis functions and this enables us to handle problems such as the Kirchhoff-Love plate and shell, where smooth coupling is an issue. Furthermore, the boundary representation within SB-IGA makes the method suitable for the concept of trimming. In particular, we see the possibility to extend the coupling procedure to study trimmed plates and shells.

The approach was implemented using the GeoPDEs package [1] and its performance was tested on several numerical examples. Finally, we discuss the advantages and disadvantages of the proposed method and outline future perspectives.

1 Summary of computational approach

First we sketch the concept of SB-IGA, then we show how to integrate the C^1 coupling across interface patches. For this purpose we introduce special basis functions for the approximation in the scaling center. Finally, we point out opportunities for generalization including trimmed geometries.

1.1 Scaled boundary isogeometric analysis

The underlying idea of SB-IGA, see e.g. [5], [6], fits to the fact that in CAD applications the computational domain is often represented by means of its boundary. For a star-convex domain Ω one chooses a scaling center $\boldsymbol{x}_0 \in \mathbb{R}^d$ and the domain is then defined by a scaling of the boundary w.r.t. to $\boldsymbol{x}_0$. In the planar case, which is the one we focus on here, and in view of the isogeometric analysis we have some boundary NURBS curve $\gamma(\zeta) = \sum_{i=1}^{n_1} \boldsymbol{C}_i \, \hat{N}_{i,p}^r(\zeta)$ and define the SB parametrization of Ω through

$$\boldsymbol{F}\colon \widehat{\Omega} \coloneqq (0,1)^2 \to \Omega \, , \; (\zeta, \xi) \mapsto \xi \, \big(\gamma(\zeta) - \boldsymbol{x}_0\big) + \boldsymbol{x}_0 .$$

Above, $\hat{N}_{i,p}^r$ denote the basis functions corresponding to a NURBS space N_p^r of degree p and global regularity C^r and they are associated to proper control points $\boldsymbol{C}_i \in \mathbb{R}^2$.

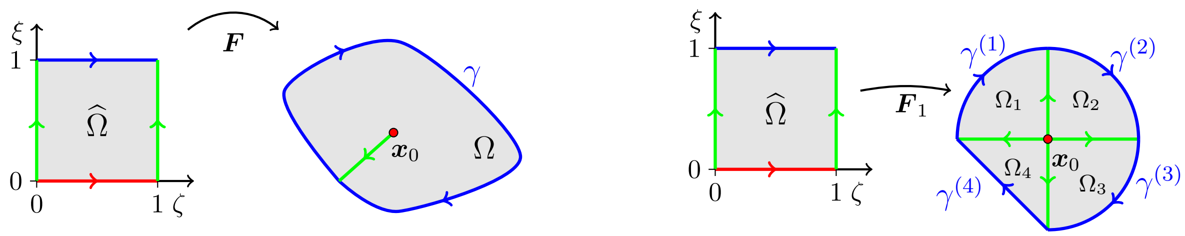

Fig. 1: On the left we have a single-patch SB parametrization and a multi-patch domain on the right. The C^1 coupling of the basis functions in the latter case requires a special consideration.

Such a SB parametrization can be interpreted as an element of a suitable NURBS space $(N_p^r \otimes S_p^r)^2$ with S_p^r denoting an univariate B-spline space. Following the concept of isogeometric analysis one introduces discrete spaces on the domain Ω by

* Corresponding author: e-mail arf@rhrk.uni-kl.de,

means of a push-forward operation, i.e. we deal with spaces of the form

$$V_h := \{\phi \,|\phi \circ \boldsymbol{F} \in N_p^r \otimes S_p^r\}.$$

However, in general the domain boundary is prescribed by multiple boundary curves; see Fig. 1. Then supposing SB parametrizations $\boldsymbol{F}_k \colon \widehat{\Omega} \to \Omega_k$ for the patches Ω_k, the uncoupled multi-patch spaces are straightforwardly given by $V_h^M := \{\phi\colon \Omega \to \mathbb{R}\, |\phi_{|\Omega_k} \in V_h^{(k)},\ \forall k\}$, where $V_h^{(k)}$ stands for the k-th patch space and $\overline{\Omega} = \cup_k \overline{\Omega_k}$. A basic assumption of our approach is the conforming patch interface property, which requires matching control points of meeting patches. Obviously, depending on the application one needs test and ansatz functions with a specific regularity. Whereas a continuous coupling, meaning spaces $V_h^0 := V_h^M \cap C^0(\Omega)$, can be achieved easily within SB-IGA, the situation becomes more difficult if higher regularity is requested.

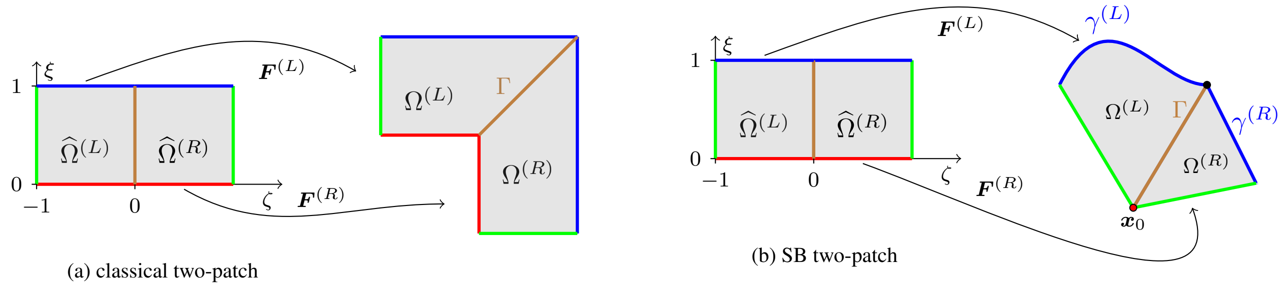

(a) classical two-patch (b) SB two-patch

Fig. 2: Compared to a classical two-patch geometry on the left we get a singularity at $\boldsymbol{x}_0$ in the SB context. In return we obtain a geometry that is closely related to so-called analysis-suitable G^1 parametrizations.

1.2 C^1 coupling

Here we look at the construction of globally C^1 smooth basis functions. In other words we focus on $V_h^1 := V_h^M \cap C^1(\Omega)$ which implies $r \geq 1, p \geq 2$. Starting point of our considerations is the work by Collin et al. [2] which coined the theoretical foundation for the C^1 coupling of isogeometric spaces. It turns out that the constraints coming along with the C^1 condition are in general too restrictive and one observes C^1 locking i.e. the worsening or loss of convergence in numerical applications. Nevertheless, for the class of analysis-suitable G^1 multi-patch (ASG^1) parametrizations these order reductions can be avoided. In the case of a simple two-patch scenario like in Fig. 2 (a) one has a ASG^1 parametrization if we find polynomial functions $\alpha^{(S)},\ \beta^{(S)}\colon [0,1] \to \mathbb{R},\ S \in \{L,R\}$ of degree at most 1 s.t.

$$\alpha^{(R)}(\xi)\,\partial_\zeta \boldsymbol{F}^{(L)}(0,\xi) - \alpha^{(L)}(\xi)\partial_\zeta \boldsymbol{F}^{(R)}(0,\xi) + \beta(\xi)\,\partial_\xi \boldsymbol{F}^{(L)}(0,\xi) = \boldsymbol{0},$$

with $\beta = \alpha^{(L)}\,\beta^{(R)} - \alpha^{(R)}\,\beta^{(L)}$. Contribution [2] states that for B-spline parametrizations latter condition guarantees enough interface functions in V_h^1 for $p > r+1 > 1$ and C^1 locking is not an issue. Thus, it is natural to prefer these special geometry representations if smoothness is crucial. An analogous two-patch geometry within SB-IGA, see Fig. 2 (b), fulfills the ASG^1 condition except at the scaling center, where a singularity appears. However, this connection between SB-IGA and ASG^1 geometries suggests good approximation properties of V_h^1 and since w.l.o.g. the NURBS weight functions are constant along SB interfaces, the SB-IGA ansatz seems appropriate for coupling also for general NURBS boundary curves.
But, on the one hand, we have to clarify how one constructs C^1 basis functions in the scaling center. On the other hand, the actual implementation of the coupling conditions should be practicable. Regarding the former, we can exploit the isoparametric paradigm observing that in $2D$ we only need three scaling center basis functions that determine the value and the first derivatives at $\boldsymbol{x}_0$. Let the k-th patch be parametrized through $\boldsymbol{F}_k(\zeta,\xi) = \sum_{i=1,j=1}^{n_1,n_2} \boldsymbol{C}_{ij}^{(k)}\, \hat{N}_{i,p}^r(\zeta)\hat{B}_{j,p}^r(\xi)$. Then we can define

$$\phi_{l,sc}^{(k)} := \hat{\phi}_{l,sc}^{(k)} \circ \boldsymbol{F}_k^{-1} \qquad \text{with} \qquad \hat{\phi}_{l,sc}^{(k)}(\zeta,\xi) := \sum_{j=1}^{p+1}\sum_{i=1}^{n_1} (\boldsymbol{C}_{ij}^{(k)})_l\, \hat{N}_{i,p}^r(\zeta)\,\hat{B}_{j,p}^r(\xi),\ \ l \in \{1,2\},$$

$$\phi_{3,sc}^{(k)} := \hat{\phi}_{3,sc}^{(k)} \circ \boldsymbol{F}_k^{-1} \qquad \text{with} \qquad \hat{\phi}_{3,sc}^{(k)}(\zeta,\xi) := \sum_{j=1}^{p+1} \hat{B}_{j,p}^r(\xi).$$

And since

$$\phi_{3,sc}(\boldsymbol{x}_0) = 1,\ \partial_m \phi_{3,sc}(\boldsymbol{x}_0) = 0 \quad \text{and} \quad \partial_m \phi_{l,sc}(\boldsymbol{x}_0) = \delta_{ml} \ \text{ for } \ l,m \in \{1,2\},$$

where the $\phi_{i,sc}$ are defined by $\left(\phi_{i,sc}\right)_{|\Omega_k} = \phi_{i,sc}^{(k)}$, we see directly that the global mappings $\phi_{i,sc}$ determine a linearly independent Hermite data set in $\boldsymbol{x}_0$.
For the implementation of the coupling conditions one can adapt the approach from [2] which results for two-patch geometries in the following steps.

1. Remove basis functios with non-vanishing values or derivatives at $\boldsymbol{x}_0$.
2. Add the scaling center basis functions $\phi_{i,sc}$.
3. Do a C^0 coupling step, i.e. we obtain globally continuous basis functions ϕ_i^0.
4. Incorporate possible boundary conditions.
5. Compute C^1 coupled basis functions by means of the null space of the interface derivative jump matrix

$$(M_J)_{i,j} = \langle [\![\nabla\phi_i^0 \cdot \boldsymbol{n}_L]\!], [\![\nabla\phi_j^0 \cdot \boldsymbol{n}_L]\!]\rangle_{L^2(\Gamma)}, \forall\phi_i^0,\ \forall\phi_j^0\ ,$$

with $\boldsymbol{n}_L$ as the normal to the interface Γ and $[\![\cdot]\!]$ as the jump at Γ. The generalization to multi-patch geometries is straightforward and consequently various shapes Ω are feasible.

1.3 Brief remarks on generalizations

Up to now our approach is quite restrictive since we assumed star-convex domains. But this restriction can be overcome. If Ω is not star-shaped we need a decomposition into star-convex blocks, which is possible e.g. utilizing a quadtree partition. Provided that the different star-convex blocks are separated by straight interfaces, like in Fig. 3 (a), we preserve the (quasi) ASG^1 structure, because the parametrizations of two blocks meet as two bilinear B-spline patches, which are always ASG^1; see Fig. 3 (b).
Another feature we want to emphasize is the possibility to construct C^1 basis functions also on trimmed geometries. Although trimming is a fundamental operation in CAD in general it comes along with several difficulties. But if we use a scaled boundary representation of the computational domain we can reduce the trimmed geometry Ω_T to a new untrimmed one in an exact manner. For this purpose we follow the steps from Fig. 4, namely

1. Compute the intersections between untrimmed boundary curves and the trimming curve γ_T; see Fig. 4(a).
2. Insert knots at the parameter values of the intersections s.t. the NURBS are discontinuous at the intersections. As a result we can extract the NURBS that are relevant for the trimmed domain representation; compare Fig. 4(b).
3. In case of star-convexity of Ω_T one calculates a new scaling center, otherwise a preliminary decomposition step has to be applied; see Fig. 4(c).

After the mentioned steps, we can couple the basis functions analogous to the untrimmed setting.

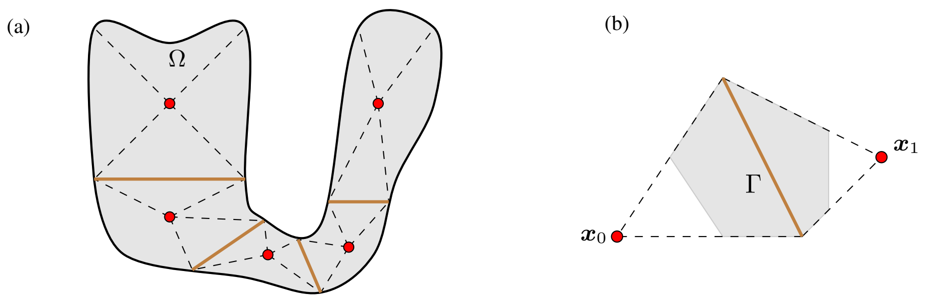

Fig. 3: To handle more complex geometries, we partition Ω in several simple star-shaped elements; see (a). If we have straight interfaces, we can assume bilinear parametrizations at block interfaces; compare (b).

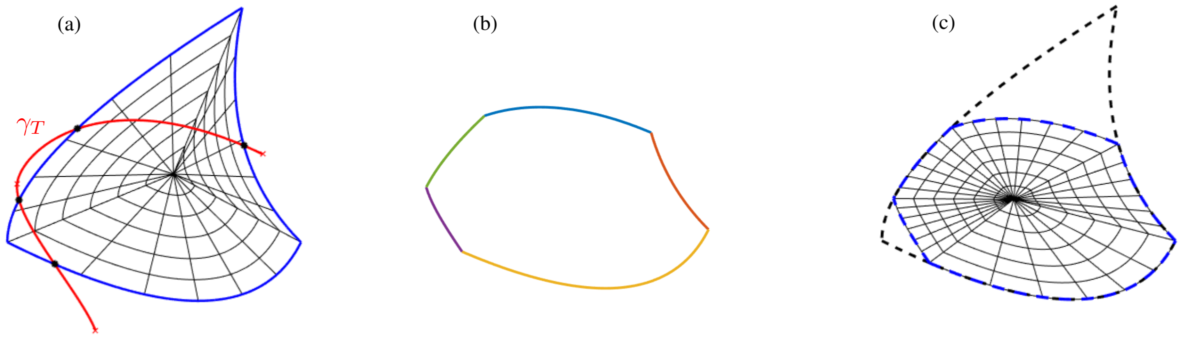

Fig. 4: Trimming can be incorporated into planar SB-IGA.

2 Numerical examples

There are different application examples and methods where C^1-regularity of test and ansatz functions is required for the numerical calculations. In this context, application examples of Kirchhoff-Love plates in structural mechanics are evaluated and discussed to show the formulations power and applicability. Kirchhoff-Love plates are a two-dimensional fourth-order boundary value problem governed by the bi-Laplace operator. Considering a domain $\Omega \subset \mathbb{R}^2$ that has a sufficient smooth boundary $\partial\Omega$ such that the unit normal vector $\mathbf{n}$ is well-defined in each point. The bilaplacian problem is stated in the strong form as

$$\Delta\Delta u = \frac{p}{D} =: g \quad \text{in} \quad \Omega, \qquad u = 0 \quad \text{on} \quad \partial\Omega \qquad \text{and} \qquad \nabla u \cdot \mathbf{n} = 0 \quad \text{on} \quad \partial\Omega,$$

with the bending stiffness $D = \frac{Et^3}{12(1-\nu^2)}$. The classical weak form of the problem for a suitable test function space $\mathcal{V}_h$ that depends on the boundary conditions reads:

$$\text{Find} \quad u_h \in \mathcal{V}_h \quad \text{s.t.} \quad \int_\Omega \nabla(\nabla u_h) : \nabla(\nabla v_h)\, d\Omega = \int_\Omega g v_h\, d\Omega, \quad \forall v_h \in \mathcal{V}_h.$$

The discretization of the solution field, meaning the definition of $\mathcal{V}_h$, is performed by the previously defined SB-IGA test functions V_h^1 including the coupling approach at the patch boundaries, which ensure C^1-continuity within the whole domain that is required for the plate formulation. In the following, the theory is applied to a rotational symmetric plate, to combine the power of the boundary representation and the exact approximation of the geometry and solution field for a circular plate, both. Afterwards, the application of trimming in scaled boundary is evaluated by trimming the center of the structure to a ring.

2.1 Rotational symmetric plate

At first, the plate formulation is checked on its general performance. A rotational symmetric plate of Ω with radius $R = 2$ is subjected to a smoothly distributed source function g that is chosen such that the exact solution is $u = \cos(\pi\,\rho/4)^2$, with ρ denoting the radial coordinate. A homogeneous and isotropic plate of elastic material with Young's modulus $E = 10^6$ and Poisson's ratio $\nu = 0$ is considered and the thickness is chosen as $t \approx 0.0229$ such that $D = 1$. The Dirichlet boundary conditions are clamped on the whole boundary of the domain. The body is discretized with four SB-IGA patches. The scaling center is placed in the center of the plate. Fig. 5 exemplary shows the mesh for $h = 1/4$ and the corresponding deformation plot.

The example is evaluated in terms of the H^2 seminorm and the L^2 norm. The results are shown in Fig. 6. The model shows good results for all orders and converges smoothly towards the reference solution. Furthermore, the convergence rate coincides for both error estimations with the optimal convergence rate $C \cdot h^{p-1}$ for the H^2 seminorm and $C \cdot h^{p+1}$ for the L^2 norm. Note that C differs for each order and error estimation.

2.2 Trimmed plate - ring

In the second example, the rotational symmetric plate from 2.1 is trimmed by a circular trimming curve defined entirely inside the domain. The resulting ring is subjected to a uniform load $g = 1$. All other properties stay the same. Since the structure is not inherently star shaped, the ring is divided manually into four star shaped domains, having four scaling centers. Consequently, the C^1 condition needs to be fulfilled also across block interfaces. The reference solution of the deformation in

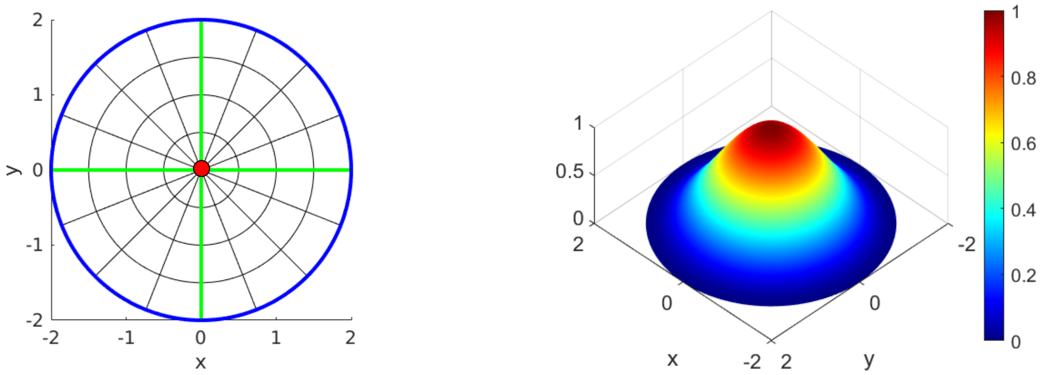

Fig. 5: Example of the smooth solution on a disk. On the left, the underlying mesh of $h = 1/4$ is pictured. On the right side, the corresponding deformation plot of the problem for the left mesh with $p = 3$, $r = 1$ is shown.

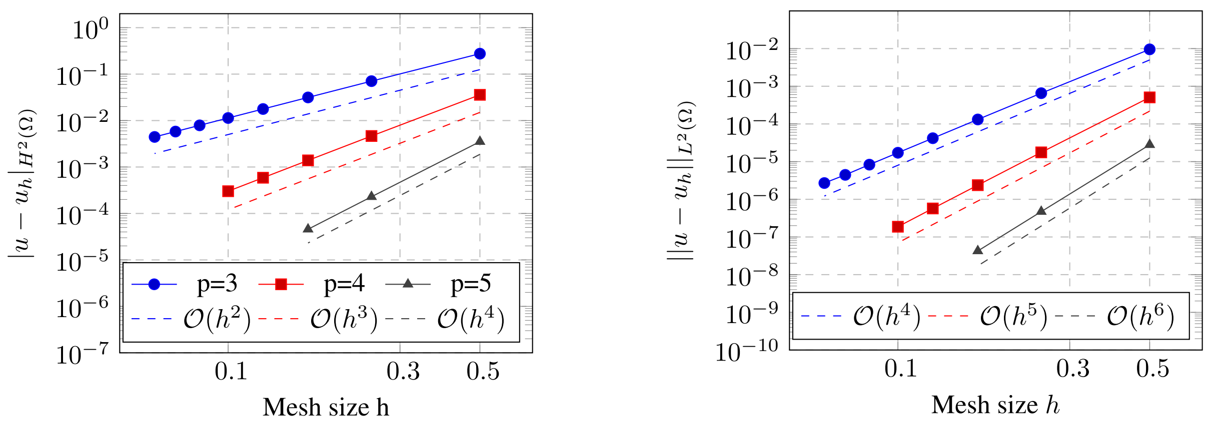

Fig. 6: Convergence studies of the H^2 seminorm errors and the L^2 errors on the example of the smooth solution on a disk and orders of $p = 3$, $p = 4$ and $p = 5$. The underlying regularity is $r = 1$, i.e. we have C^1 smooth splines within each patch.

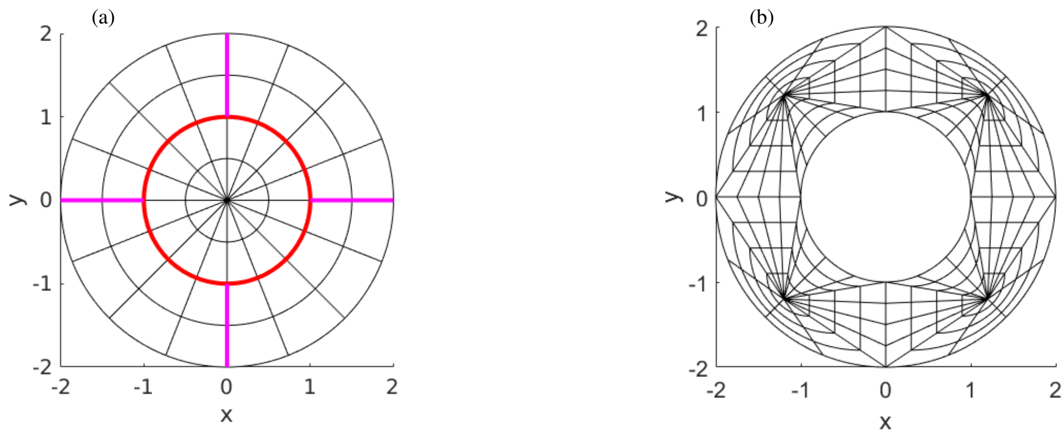

Fig. 7: On the left, the original disk mesh for $h = 1/4$ is pictured including the trimming curve (red) and cut lines (magenta) which are used to obtain the SB mesh for the ring on the right.

radial direction using a Kirchhoff approach for rotational symmetric plates yields a smooth solution w.r.t. the radial variable ρ. The results show that the trimming is applicable and the trimmed geometry is described properly. Moreover, in Fig. 8 the corresponding deformation plot for the mesh from Fig. 7 (b) is displayed, also along the radial direction. The results show good agreement with the analytical solution.

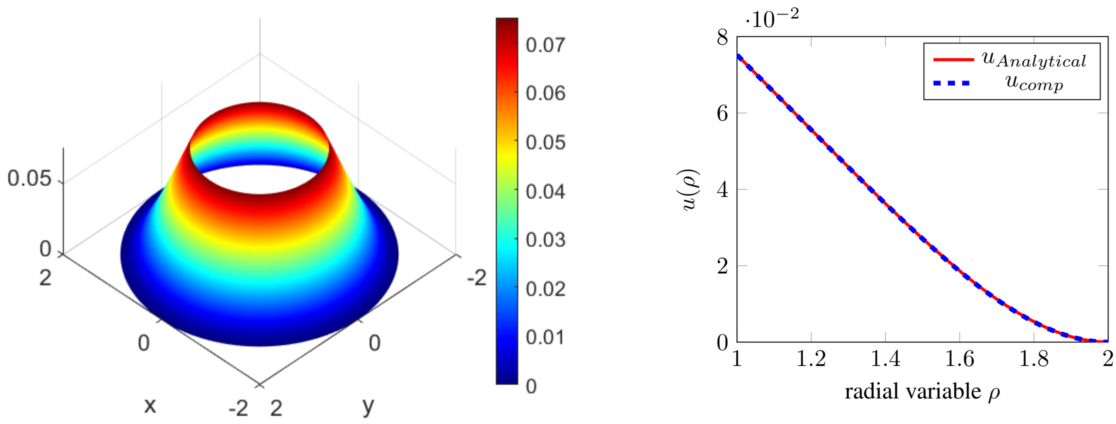

Fig. 8: The corresponding deformation plot of the mesh figured above and the comparison of the computed deflection in radial direction along the cut line with $y = 0$ is shown; $(p = 4,\ r = 1)$.

3 Conclusion and outlook

We showed that C^1 coupling in the context of SB-IGA is possible, despite the singularity in the scaling center. Since the underlying parametrizations fit to the class of ASG^1 geometries from [2], we should not suffer from C^1 locking which is also confirmed by different numerical experiments. Still there are different aspects which are objects of ongoing research, which should be considered in the future, respectively. First of all, we think that the C^1 coupling is appropriate to study also (trimmed) Kirchhoff-Love shells [3], [4]. For this purpose, one applies the coupling in the planar parametric domain of the shell and uses the C^1 basis functions to approximate the geometry as well as the shell displacement. On the downside of our approach we have the restriction of conforming patch interfaces. Another point is the need of additional stabilization in case of fine SB meshes as the mesh elements near the scaling center degenerate.

Acknowledgements The financial support of the DFG (German Research Foundation) under Grant No. KL1345/10-2 is gratefully acknowledged. Open access funding enabled and organized by Projekt DEAL.

References

[1] C. de Falco, A. Reali and R. Vázquez, Adv. Eng. Softw. **42**, 1020-1034 (2011).
[2] A. Collin, G. Sangalli and T. Takacs, Comput. Aided Geom. Des. **47**, 93-113 (2016).
[3] J. Kiendl, K. U. Bletzinger, J. Linhard and R. Wüchner, Comput. Methods in Appl. Mech. Eng. **198**, 3902-3914 (2009).
[4] L. Coradello, P. Antolin, R. Vázquez and A. Buffa, Comput. Methods in Appl. Mech. Eng. **364**, 3902-3914, (2020).
[5] C. Arioli, A. Shamanskiy, S. Klinkel and B. Simeon, Comput. Methods in Appl. Mech. Eng. **349**, 576-594, (2019).
[6] M. Chasapi and S. Klinkel, Comput. Methods in Appl. Mech. Eng. **333**, 475-496, (2018).

